Magnetic and magneto-optical properties of bismuth-substituted lutetium iron garnet films

P. Hansen, C.-P. Klages, J. Schuldt, and K. Witter
Philips GmbH Forschungslaboratorium Hamburg, D-2000 Hamburg 54, Federal Republic of Germany
(Received 17 December 1984)

Epitaxially grown bismuth-substituted lutetium iron garnet films of composition $Lu_{3-x}Bi_xFe_5O_{12}$ and $(Lu,Y)_{3-x}Bi_xFe_5O_{12}$ have been investigated with respect to the bismuth-induced changes of the saturation magnetization M_s, the Curie temperature T_C, the growth-induced anisotropy K_u^g, the optical absorption α, and the Faraday rotation θ_F. The composition and temperature dependence of M_s and θ_F at $\lambda=633$ nm have been measured in the range $0\leq x\leq 2.17$ and $4.2\ \mathrm{K}\leq T\leq T_C$, respectively, revealing basically the same dependences on x as observed for bismuth-substituted yttrium and gadolinium iron garnet films. In contrast to the latter compositions, K_u^g turns out to be much smaller in lutetium-bismuth iron garnet films and is significantly increased by small yttrium additions. The temperature dependence of θ_F can be described in terms of the sublattice magnetizations using constant magneto-optical coefficients. The measured temperature dependence of K_u^g is compared with calculated results based on the single-ion theory.

I. INTRODUCTION

Lutetium and bismuth substitutions in epitaxially grown iron garnet films have been used to control both the magnetic and magneto-optical properties and the lattice constant. In particular, the strong influence of the bismuth on the superexchange interaction, the effective spin-orbit coupling, and the local crystalline fields and its nonuniform distribution on dodecahedral sites cause a pronounced increase of the Curie temperature, the optical and magneto-optical effects, and the uniaxial anisotropy. In certain limits these properties can be varied independently using a proper choice of the composition and the growth conditions which make such films attractive candidates for various applications such as bubble[1–4] or magneto-optical[5–9] devices. The influence of the bismuth on the magnetic and magneto-optical properties have been focused essentially on yttrium- (Refs. 10–15) and gadolinium- (Refs. 13 and 15–17) based garnets. For bismuth-substituted lutetium iron garnet films, however, very few data are available, except for some investigations concerning primarily the growth-induced anisotropy.[2,4,18–20] In the present work, therefore, we have investigated films of composition $R_{3-x}Bi_xFe_5O_{12}$ (R=Y,Lu) with respect to the compositional and temperature dependence of the magnetic and magneto-optical properties. The experimental data are compared with theoretical results based on the molecular-field theory and the single-ion theory.

II. EXPERIMENTAL RESULTS

A. Garnet material characterization

Garnet films of composition

$$Lu_{3-x-y}Bi_xPb_yFe_{5-z}Pt_zO_{12}$$

and

$$(Y,Lu)_{3-x-y}Bi_xPb_yFe_{5-z}Pt_zO_{12}$$

were grown by liquid-phase epitaxy onto [111]-oriented rare-earth gallium garnet or onto Ca-, Mg-, or Zr-substituted gadolinium gallium garnet substrates.[21] The films were grown from a supersaturated melt applying the horizontal dipping mode and a rotation rate of 90 rpm. The sign of rotation was reversed every six revolutions. Different melt compositions and growth conditions were used[19] to control the bismuth content and to affect its distribution on dodecahedral sites. The maximum bismuth content achieved in Lu-Bi films is about 1.5. Higher values have been realized in (Y,Lu)-Bi films. The analysis data, lattice constant a, film thickness t, and supercooling ΔT_s are compiled in Table I for those films selected for the temperature-dependence measurements. The lead and the platinum enter the crystal as impurities. The lead and the bismuth content are primarily determined by ΔT_s. The film lattice constants determined from the lattice mismatch measured with an x-ray diffractometer using a Cu $K\alpha$ reflection and the substrate lattice constants increase linearly with the bismuth content yielding approximately $a\simeq a_0(1+0.0095x)$ where $a_0=1.2287$ nm. The film thickness has been deduced from the reflection spectra in the wavelength range between 1000 and 2000 nm. The strong influence of the bismuth on the refractive index[15,22] n has been taken into account using the empirical relation

$$n(\lambda,x)=2.174+0.0593\lambda^{-2}+(0.103+0.0371\lambda^{-2})x \quad (1)$$

applying approximately to the long-wavelength region of a single transition ϕ and λ is expressed in μm. This equation is also valid for other rare-earth–bismuth iron garnets since to first approximation n remains constant for all rare-earth iron garnets.[23] At $\lambda=1152$ nm the bismuth-induced change of n is $\Delta n/x=0.13$ which is in agreement with data reported for $(Y,Lu)_{3-x}Bi_xFe_5O_{12}$ garnet films.[24]

TABLE I. Supercooling ΔT_s, chemical analysis data, lattice constant a, and film thickness t of epitaxial garnet films of composition $Lu_{3-x-y}Bi_xPb_yFe_{5-z}Pt_zO_{12}$ and $(Lu,Y)_{3-x-y}Bi_xPb_yFe_{5-z}Pt_zO_{12}$.

Sample	ΔT_s (K)	x	y	z	a (nm)	t (μm)
1	4	0	0.014	0.019	1.2287	1.2
2	35	0	0.053	0.035	1.2297	3.2
3	4	0.09	0.010	0.022	1.2297	2.5
4	28	0.18	0.025	0.039	1.2310	5.2
5	5	0.53	0.020	0.022	1.2340	2.3
6	37	0.99	0.031	0.021	1.2395	2.6
7	57	1.31	0.045	0.028	1.2437	3.9
8[a]	40	1.40	0.044	0.022	1.2435	4.4
9		1.48	0.050	0.024	1.2453	2.0
10[a]	124	1.57	0.037	0.023	1.2469	3.6
11[a]		1.67	0.033	0.027		2.3
12[a]	150	1.81	0.050	0.024	1.2505	2.9
13[a,b]		2.17	0.034	0.024	1.2499	3.7
Error	±2	±0.03	±0.01	±0.005	±0.001	±5%

[a]Samples 8, 10, 11, 12, and 13 contain an yttrium concentration of 0.33, 0.71, 0.70, 0.63, and 0.57 at. %, respectively.
[b]This sample contains 0.53 at. % aluminum.

B. Magnetic properties

1. Saturation magnetization

The saturation magnetization M_s was measured with a vibrating sample magnetometer in fields up to 1.6×10^6 $A\,m^{-1}$. The M_s data are obtained from extrapolation to zero field. The temperature dependence of the saturation polarization $I_s=\mu_0 M_s$ is shown in Fig. 1 for three compositions, indicating a small decrease of I_s towards increasing x at low temperatures and an increase of I_s at high temperatures due to the rise of the Curie temperature. The low-temperature M_s data are influenced by the impurity content, the fraction of lutetium ions on octahedral sites, and the bismuth content causing an increase of the lattice constant. For "pure" lutetium iron garnet (sample 1) the analysis data reveal a fraction of 0.03 lutetium on octahedral sites, explaining the value of $I_s=210$ mT at $T=0$ K which implies for the Fe^{3+} moment $g\mu_B S=5\mu_B$. Here g, S, and μ_B are the Landé factor, the spin quantum number, and the Bohr magneton, respectively. The higher iron moment reported for polycrystalline lutetium iron garnet[25] has been presumably attributed also to a small amount of octahedral lutetium as it has been observed for other lutetium-containing iron garnets.[18,26] The solid lines in Fig. 1 have been calculated in terms of the molecular-field theory,

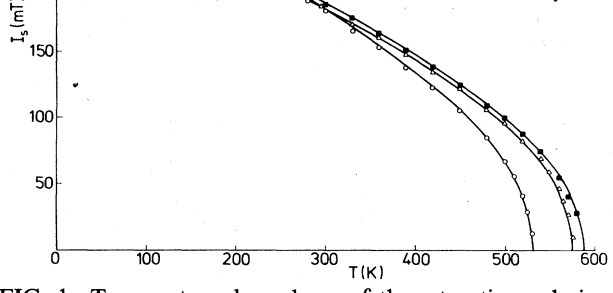

FIG. 1. Temperature dependence of the saturation polarization $I_s=\mu_0 M_s$ for lutetium-bismuth iron garnet films. The solid lines were calculated applying the molecular-field theory.

$$M_i(x,T)=M_i(0,T)B_S(z_i)\,,$$
$$z_i(x,T)=\frac{g\mu_B S}{kT}[\lambda_{ii}M_i(x,T)+\lambda_{ij}M_j(x,T)]\,, \tag{2}$$

where $B_S(z_i)$, $M_i(x,T)$, and k are the Brillouin function, the tetrahedral ($i,j=d$) and octahedral ($i,j=a$) sublattice magnetizations, and the Boltzmann constant, respectively. The molecular-field coefficients are obtained from the fit of Eq. (2) to the measured temperature dependences of M_s for various bismuth concentrations, yielding

$$\lambda_{aa}=-29.4\,,$$
$$\lambda_{dd}=-65.5\,, \tag{3}$$
$$\lambda_{ad}=94.7(1+0.04x)\,.$$

The λ_{ik} are expressed in mole cm^{-3}. The dependence of λ_{ad} on x reflects the increase of the Curie temperature T_C by the bismuth owing to its influence on the superexchange interaction. The variation of T_C with x is displayed in Fig. 2. The value for $Lu_3Fe_5O_{12}$ is found to be $T_C=531$ K, in good agreement with $T_C=530$ K reported for a polycrystalline sample.[27] The slope of the straight line $\Delta T_C/x\simeq42$ K results in being slightly larger than that found for yttrium- (dashed line) and gadolinium-bismuth iron garnets.[10,14,15,17]

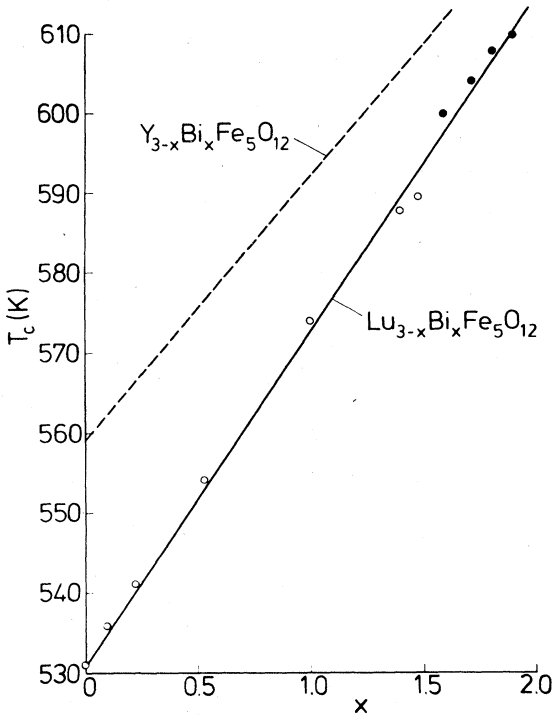

FIG. 2. Curie temperature vs bismuth content. The solid circles represent films containing yttrium.

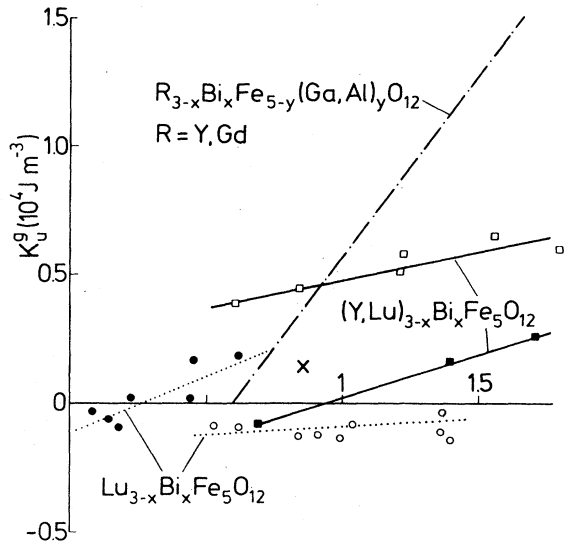

FIG. 3. Growth-induced uniaxial anisotropy constant vs bismuth content at $T=295$ K for [111]-oriented films. The slope of the dashed-dotted line representing Y-Bi and Gd-Bi films depends strongly on the growth conditions (Refs. 14 and 20). The Lu-Bi films represented by the open and solid circles have been grown from melts described in Refs. 19 and 18, respectively.

2. *Uniaxial anisotropy*

The incorporation of bismuth in yttrium and gadolinium iron garnet films gives rise to large uniaxial anisotropies, depending on the bismuth content and the growth conditions.[1–4,14,17–20,28] For lutetium-bismuth iron garnet films different results have been reported concerning the magnitude of the uniaxial anisotropy constant K_u.[1,4,18–20,29] The films of composition $Lu_{3-x}Bi_xFe_5O_{12}$ and $(Lu,Y)_{3-x}Bi_xFe_5O_{12}$ investigated in this work have been grown under different growth conditions[19] revealing low or moderate K_u values.

The K_u data of the [111]-oriented films have been measured with the torque method. These data were corrected for mismatch strain according to a standard relation involving the magnetostrictive constant λ_{111}, Young's modulus E, and Poisson's ratio μ [for $Y_3Fe_5O_{12}$ at $T=295$ K (Refs. 14 and 30): $\lambda_{111}(x)=\lambda_{111}(0)\,(1+0.23x)$ with $\lambda_{111}(0)=-2.73\times10^{-6}$ (Refs. 31 and 32), $E=2.055\times10^{11}$ J m^{-3}, $\mu=0.30$]. The temperature dependence of λ_{111} has been taken into account using data obtained from bulk crystals.[14] The resulting growth-induced anisotropy constant K_u^g is plotted in Fig. 3 as a function of x for films grown from different melt compositions. The Lu-Bi films (open and solid circles) are characterized by small positive or even negative K_u^g values. This applies also to those films grown from the melt composition given in Ref. 18 (solid circles). In that paper large uniaxial anisotropies are found exhibiting no dependence of K_u^g on additions of yttrium. Our films show a significant increase of K_u^g when yttrium is added (open and solid squares) but even then the absolute magnitude of K_u^g and the slope of the linear dependences are much lower than those reported in Ref. 18 and for Y-Bi and Gd-Bi films. The reason for the different anisotropy of the films grown by almost the same growth conditions is still unaccounted for.

The magnitude of K_u^g and its temperature dependence is controlled by the bismuth-induced change of the atomic parameters determining the energy levels of the Fe^{3+} ions on octahedral and tetrahedral sites and by the preferential ordering of the Bi^{3+} ions on the dodecahedral sites along the growth direction. This influence of the Bi^{3+} ions has been studied recently,[33,34] leading to a uniaxial anisotropy of the form

$$K_u^g(x,T)=c_a(x)p_a(x,T)+c_d(x)p_d(x,T)\ . \tag{4}$$

$p_i(x,T)$ is determined by the energy-level splitting governed by the exchange energy and the local axial crystalline-field energy. For [111] films the coefficients $c_i(x)$ are proportional to the difference of the occupation probabilities of the two classes of dodecahedral sites and to the bismuth-induced change of the axial-field parameters. $p_i(x,T)$ can be expressed in terms of the sublattice magnetizations by[35]

$$\begin{aligned} p_i(x,T)&=Z_0^{-1}(5-y_i-4y_i^2-4y_i^3-y_i^4-5y_i^5)\ , \\ \frac{M_i(x,T)}{M_i(0,T)}&=(5Z_0)^{-1}(5+3y_i+y_i^2-y_i^3-3y_i^4-5y_i^5)\ , \end{aligned} \tag{5}$$

where $y_i=\exp(-g\mu_B H_{\rm exch}^{(i)}/kT)$ and $Z_0=\sum_{p=1}^{n} y_i^p$.

The coefficients $c_i(x)$ cannot be calculated at present

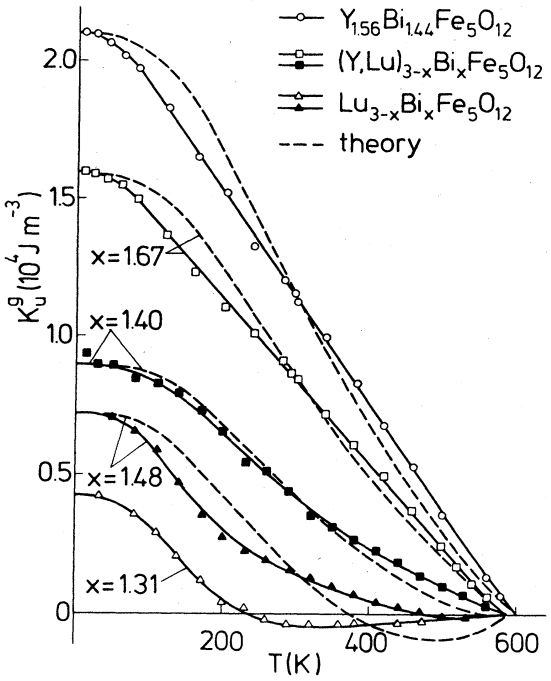

FIG. 4. Temperature dependence of the growth-induced uniaxial anisotropy constant for [111]-oriented films. The dashed lines have been calculated from the single-ion theory.

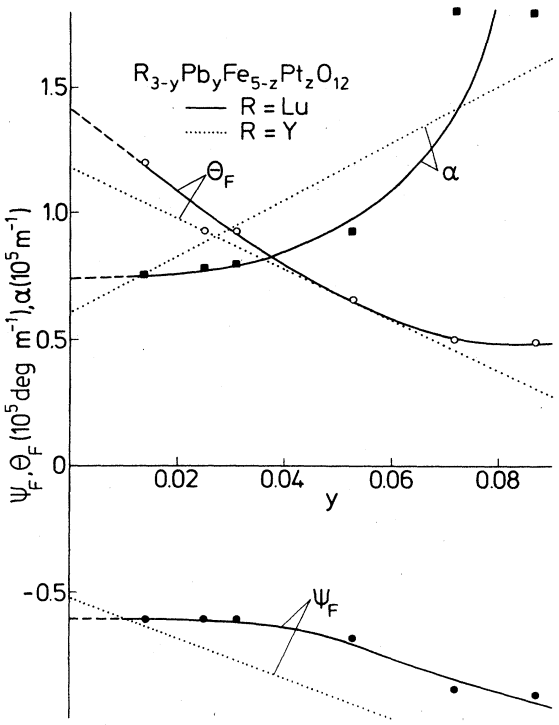

FIG. 5. Faraday rotation θ_F, Faraday ellipticity ψ_F, and optical absorption x vs lead content at $\lambda=633$ nm and $T=295$ K.

and must be considered as adjustable parameters. The sublattice magnetizations can be inferred from the fit of the molecular-field theory to the measured saturation magnetization using Eqs. (2) and (3). The measured and calculated temperature dependences of K_u^g are displayed in Fig. 4 for films of composition $R_{3-x}Bi_xFe_5O_{12}$ with R=Y, Lu, or (Y,Lu). The theoretical curves have been adjusted at $T=0$ and 295 K. For Y-Bi and (Y,Lu)-Bi films a satisfactory agreement between theory and experiment can be achieved which applies also to films with other orientations.[20] The measured temperature variation of K_u^g for Lu-Bi films is characterized by a faster reduction at low temperatures leading to a higher deviation between theory and experiment. This may be associated with a stronger lattice distortion as compared to that of Y-Bi and Gd-Bi films. In this case the fourth-order terms in the spin Hamiltonian may be important.

C. Magneto-optical properties

The growth of garnet films from a lead-containing melt implies the presence of more or less Pb^{2+} ions in the crystal affecting the optical and magneto-optical properties.[14,36–38] This applies in particular to the optical absorption α, the Faraday rotation θ_F, and the Faraday ellipticity ψ_F, which are shown in Fig. 5 as a function of the lead content at $\lambda=633$ nm and $T=295$ K. For Lu-Pb films a deviation from linearity occurs already at very low y while Y-Pb films (dotted lines) exhibit a linear dependence up to $y\approx0.2$ (Ref. 14). This difference is presumably associated with the different influence of the band-edge shift with increasing y on these properties at $\lambda=633$ nm and possibly also with a different charge-compensation mechanism. The rotation and absorption of a lead-free lutetium (yttrium) iron garnet can be evaluated by extrapolation to $y=0$ yielding $\theta_F(y=0)=1.4\times10^5$ deg m^{-1} (1.2×10^5 deg m^{-1}) and 0.75×10^5 m^{-1} (0.6×10^5 m^{-1}), respectively. The reason for the higher value of $\theta_F(y=0)$ for a lutetium iron garnet as compared to an yttrium iron garnet becomes obvious from the spectral dependence of θ_F displayed in Fig. 6 at $T=295$ K for these garnets. The spectrum of the lutetium iron garnet is slightly shifted toward longer wavelengths. Its higher lead content (sample 2, $y=0.053$) causes lower θ_F values as compared to the yttrium iron garnet ($y\approx0.035$). However, in the limit $y=0$ the θ_F values of the lutetium iron garnet exhibit the higher values around $\lambda=633$ nm owing to the shifted spectral dependence.

From a plot of θ_F versus Pb^{2+} concentration $y_{Pb^{2+}}=\frac{1}{2}(y+z)$, which leads approximately to a linear dependence, the contribution $\Delta\theta_F/y_{Pb^{2+}}$ can be estimated, yielding -1.5×10^6 deg m^{-1}. This is slightly lower than that extracted for $Y_{3-y}Pb_yFe_5O_{12}$ films,[14] which is $\Delta\theta_F/y_{Pb^{2+}}\simeq-1.8\times10^6$ deg m^{-1}.

The bismuth induces a large Faraday rotation in iron garnets essentially due to strong transitions occurring around $\lambda=300$, 380, and 440 nm.[15] θ_F increases linearly with the bismuth content, as is demonstrated in Fig. 7 for $\lambda=633$ nm and $T=295$ K. The solid circles represent (Y,Lu)-Bi films. The contribution per Bi^{3+} ion $\Delta\theta_F/x\simeq-1.9\times10^6$ deg m^{-1} is slightly lower than that

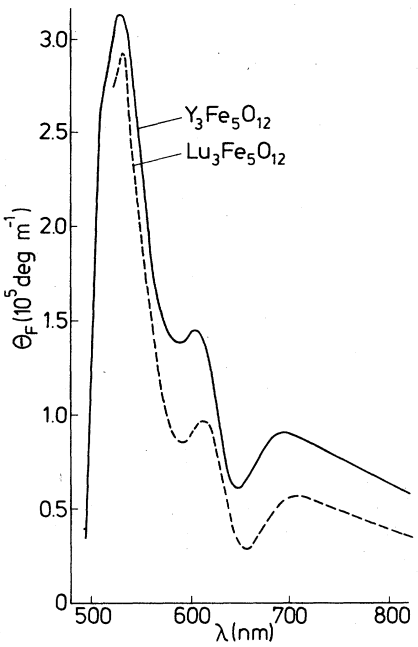

FIG. 6. Spectral dependence of the Faraday rotation for an yttrium and a lutetium iron garnet film at $T=295$ K. The lead content for these films is $y=0.035$ and 0.053, respectively.

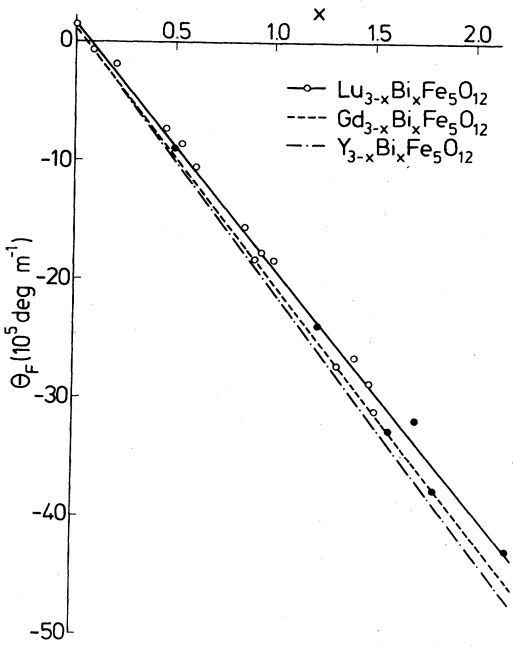

FIG. 7. Faraday rotation vs bismuth content at $\lambda=633$ nm and $T=295$ K. The solid circles refer to (Y,Lu)-Bi films.

observed for Y-Bi (Ref. 14) and Gd-Bi (Ref. 17), and (Lu,Sm)-Bi (Ref. 39), films.

The measured temperature dependence of θ_F at $\lambda=633$ nm is presented in Fig. 8 for various Lu-Bi and (Y,Lu)-Bi compositions and for $Y_3Fe_5O_{12}$. For $Lu_3Fe_5O_{12}$ and $Y_3Fe_5O_{12}$ the data reveal basically the same temperature dependence as expected from the saturation magnetization and the position of the magneto-optical transitions for these very similar garnets. The small differences of the curves arise from the different lead content and the different Curie temperature. The temperature dependence of the Faraday ellipticity ψ_F for $Lu_3Fe_5O_{12}$ and $Y_3Fe_5O_{12}$ is shown in Fig. 8(a). In the low-temperature range the shift of ψ_F towards lower values is already obvious. In the lead-free case a curvature of θ_F like that of $Y_3Fe_5O_{12}$ is expected.

The temperature dependence of θ_F is governed by the sublattice magnetizations and can be expressed in the wavelengths range sufficient away from the transitions by[40]

$$\theta_F(x,T)=A(x)M_a(x,T)+D(x)M_d(x,T)\ , \tag{6}$$

where $A(x)$ and $D(x)$ are the magneto-optical coefficients for octahedral and tetrahedral sites, respectively. Considering $A(x)$ and $D(x)$ as temperature independent and as adjustable constants $\theta_F(x,T)$ can be calculated from the sublattice magnetizations which can be inferred from the fit of the molecular-field theory to the measured saturation magnetization using Eqs. (2) and (3). The calculated dependences (dashed lines) are in good agreement with the experimental data for $Lu_3Fe_5O_{12}$ and $Y_3Fe_5O_{12}$. For the films with a higher bismuth content the agreement is less good and deviations between theory and experiment occur in the high-temperature range. For small bismuth contents ($x=0.09$ and 0.18) large deviations are present which can partly be attributed to the lead content. In this case a better description of the experimental results can be achieved with temperature-dependent coefficients or taking into account higher-order terms[41] in Eq. (6). The extracted magneto-optical coefficients reveal a nonlinear dependence on x similar to that found for $R_{3-x}Bi_xFe_5O_{12}$ with $R=$Y,Gd.[14] For $Lu_3Fe_5O_{12}$ the adjustment yields the values $A=4.62\times10^4$ and $D=-2.76\times10^4$ expressed in deg m$^{-1}\mu_B^{-1}$.

III. CONCLUSION

Bismuth-substituted lutetium-based iron garnet films of composition $R_{3-x}Bi_xFe_5O_{12}$ with $R=$Lu and (Lu,Y) and a maximum bismuth content up to 2.17 have been investigated with respect to the magnetic and magneto-optical properties. The influence of the bismuth on the superexchange affects the saturation magnetization essentially via the increase of the Curie temperature which is $\Delta T_C/x\simeq42$ K. At $T=295$ K M_s is not much changed, as in the case of $Y_3Fe_5O_{12}$. The temperature dependence of M_s can be well described in terms of the molecular-field theory implying an a-d exchange constant increasing linearly with x. The growth-induced uniaxial anisotropy constant K_u^g ranges between -10^3 and 7×10^3 J m^{-3}. The

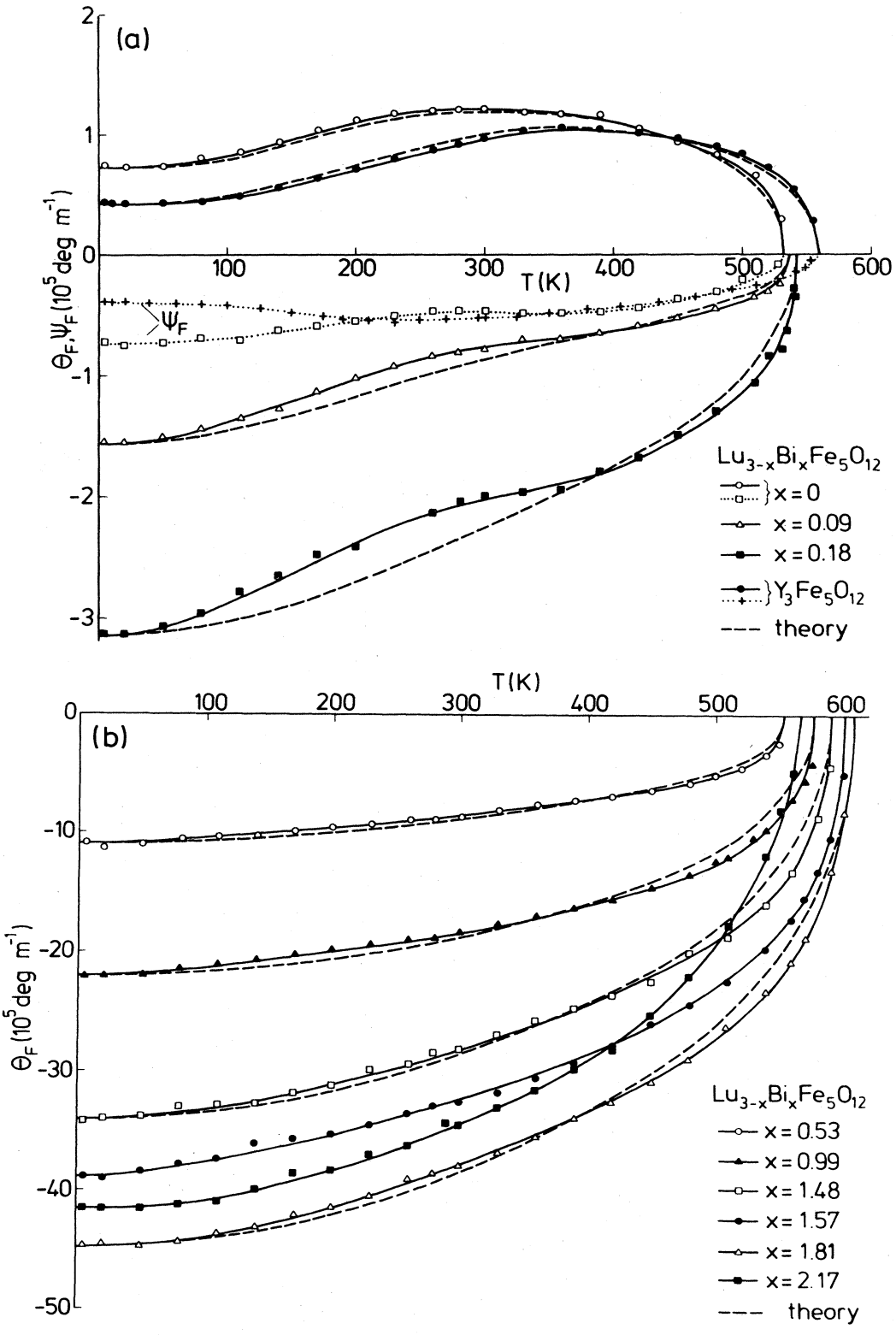

FIG. 8. Temperature dependence of the Faraday rotation at $\lambda = 633$ nm. The dashed lines were calculated using the sublattice magnetizations inferred from the fit of the molecular-field theory to the measured saturation magnetization. The samples with $x = 1.57$, 1.81, and 2.17 contain some yttrium (see Table I). The dotted lines in (a) represent the measured Faraday ellipticity for a lutetium (sample 2) and an yttrium (Ref. 14) iron garnet film.

dependence of K_u^g on x and the growth conditions are much less pronounced than for Y-Bi and Gd-Bi films. The comparison of the measured temperature dependence of K_u^g with calculated values based on the single-ion theory leads to a much less satisfactory agreement than in the case of Y-Bi films.

The influence of lead and bismuth on the optical absorption and the Faraday rotation is basically the same as in other iron garnets. The bismuth-induced rotation was found to be $\Delta\theta_F/x \simeq -1.9\times 10^6$ deg m^{-1} at $\lambda=633$ nm and $T=295$ K. The basic features of the temperature dependence of θ_F can be described in terms of the sublattice magnetizations using temperature-independent magneto-optical coefficients.

ACKNOWLEDGMENTS

The authors would like to thank P. Willich for the chemical analysis and C. Clausen and V. Doormann for magneto-optical measurements.

[1]J. M. Robertson, H. A. Algra, and D. J. Breed, J. Appl. Phys. **52**, 2338 (1981).
[2]L. C. Luther, R. C. LeCraw, J. F. Dillon, and R. Wolfe, J. Appl. Phys. **53**, 2478 (1982).
[3]Y. Hosoe, K. Andoh, N. Ohta, and Y. Sugita, J. Appl. Phys, **55**, 2542 (1984).
[4]P. Hansen, J. M. Robertson, W. Tolksdorf, and K. Witter, IEEE Trans. Magn, **MAG-20**, 1099 (1984).
[5]B. Hill and K.-P. Schmidt, Philips J. Res. **33**, 211 (1978).
[6]W. E. Ross, D. L. Cox, J. J. Fernandez de Castro, and R. Pulliman, SID Digest VIII, 98 (1982).
[7]P. Hansen, B. Hill, and W. Tolksdorf, Philips Tech. Rev. **41**, 33 (1983).
[8]B. Hill, IEEE Trans. Magn. **MAG-20**, 978 (1984).
[9]P. Paroli, Thin Solid Films **114**, 187 (1984).
[10]S. Geller, in *Physics of Magnetic Garnets,* edited by A. Paoletti (North-Holland, New York, 1978), p. 38.
[11]S. Wittekoek, T. J. A. Popma, J. M. Robertson, and P. Bongers, Phys. Rev. B **12**, 2777 (1975).
[12]D. E. Lacklison, G. B. Scott, H. I. Ralph, and J. L. Page, IEEE Trans. Magn. **MAG-9**, 457 (1973).
[13]H. Takeuchi, Jpn. J. Appl. Phys. **14**, 1903 (1975).
[14]P. Hansen, K. Witter, and W. Tolksdorf, Phys. Rev. B **27**, 6608 (1983).
[15]P. Hansen and J.-P. Krumme, Thin Solid Films **114**, 69 (1984).
[16]J. M. Robertson, S. Wittekoek, T. J. A. Popma, and P. F. Bongers, Appl. Phys. **2**, 219 (1973).
[17]P. Hansen, K. Witter, and W. Tolksdorf, Phys. Rev. B **27**, 4375 (1983).
[18]L. C. Luther, R. C. LeCraw, and F. Ermanis, J. Cryst. Growth **58**, 95 (1982).
[19]C.-P. Klages, P. Hansen, and K. Witter, IEEE Trans. Magn. **MAG-20**, 1879 (1984).
[20]P. Hansen and K. Witter, J. Appl. Phys. (to be published).
[21]D. Mateika, R. Laurien, and C. Rusche, J. Cryst. Growth **56**, 677 (1982).
[22]V. Doormann, J.-P. Krumme, and C.-P. Klages, Appl. Phys. A **34**, 223 (1984).
[23]P. K. Tien, J. R. Martin, S. L. Blank, S. H. Wemple, and L. J. Varnerin, Appl. Phys. Lett. **21**, 207 (1972).
[24]H. Moriceau, B. Ferrand, M. F. Armand, M. Olivier, D. Challeton, and J. Daval, IEEE Trans Magn. **MAG-20**, 1004 (1984).
[25]S. Geller, J. P. Remeika, R. C. Sherwood, H. J. Williams, and G. P. Espinosa, Phys. Rev. A **137**, 1034 (1965).
[26]D. M. Gualtieri, P. F. Tumelty, and M. A. Gilleo, J. Appl. Phys. **52**, 2335 (1981).
[27]A. A. Stelmach, E. E. Anderson, and S. Arajs, J. Phys. Chem. Solids **34**, 1343 (1973).
[28]P. Hansen and M. Hartmann, International Conference on Physics of Magnetic Materials, Jadwisin, Poland, 1984 [Acta Phys. Pol. (to be published)].
[29]Y. Hosoe, N. Ohta, K. Andoh, and Y. Sugita, Conference Proceedings of the Seventh Conference of the Magnetics Society of Japan, 1983 (unpublished), p. 28.
[30]P. Hansen, K. Witter, and W. Tolksdorf, J. Appl. Phys. **55**, 1052 (1984).
[31]P. Hansen, J. Appl. Phys. **45**, 3638 (1974).
[32]P. Hansen, in *Physics of Magnetic Garnets,* edited by A. Paoletti (North-Holland, New York, 1978), p. 56.
[33]P. Novák, Phys. Lett. A **104**, 293 (1984).
[34]P. Novák, Czech. J. Phys. B **34**, 1060 (1984).
[35]W. P. Wolf, Phys. Rev. **108**, 1152 (1957).
[36]K. Shinagawa, H. Takeuchi, and S. Taniguchi, Jpn. J. Appl. Phys. **12**, 466 (1973).
[37]P. Hansen, M. Rosenkranz, and K. Witter, Phys. Rev. B **25**, 4396 (1982).
[38]P. Hansen, W. Tolksdorf, and K. Witter, IEEE Trans. Magn. **MAG-17**, 3211 (1981).
[39]F. Mada and K. Yamaguchi, in Proceedings of the 30th Annual Conference on Magnetism and Magnetic Materials (San Diego, 1984), edited by R. Hasegawa, N. C. Koon, and D. L. Huber [J. Appl. Phys. **57** (1985)].
[40]W. A. Crossley, R. W. Cooper, J. L. Page, and R. P. van Stapele, Phys. Rev. **181**, 896 (1969).
[41]P. Hansen and K. Witter, Phys. Rev. B **27**, 1498 (1983).